## **TRB Annual Meeting**

# Promoting Multidimensional Equity through Collaborative Routing using Incentive Mechanisms --Manuscript Draft--

Full Title:	Promoting Multidimensional Equity through Collaborative Routing using Incentive Mechanisms
Abstract:	Penalty-based strategies, such as congestion pricing, have been employed to improve traffic network efficiency, but they face criticism for their negative impact on users and equity concerns. Collaborative routing, which allows users to negotiate route choices, offers a solution that considers individual heterogeneity. Personalized incentives can encourage such collaboration and are more politically acceptable than penalties. This study proposes a collaborative routing strategy that uses personalized incentives to guide users towards desired traffic states while promoting multidimensional equity. Three equity dimensions are considered: accessibility equity (equal access to jobs, services, and education), inclusion equity (route suggestions and incentives that do not favor specific users), and utility equity (envy-free solutions where no user feels others have more valuable incentives). The strategy prioritizes equitable access to societal services and activities, ensuring accessibility equity in routing solutions. Inclusion equity is maintained through non-negative incentives that consider user heterogeneity without excluding anyone. An envy-free compensation mechanism achieves utility equity by eliminating envy over incentive-route bundles. A constrained traffic assignment (CTA) formulation and consensus optimization variant are then devised to break down the centralized problem into smaller, manageable parts and a decentralized algorithm is developed for scalability in large transportation networks and user populations. Numerical studies investigate the model's enhancement of equity dimensions and the impact of hyperparameters on system objective tradeoffs and demonstrate the algorithm convergence.
Manuscript Classifications:	Planning and Analysis; Transportation Demand Management AEP60; Behavior Change/Behavior Science/Nudge; Congestion Pricing; Incentives/Benefits; Transportation Network Modeling AEP40; Mathematical Modeling; Optimization
Manuscript Number:	TRBAM-24-02174
Article Type:	Presentation
Order of Authors:	Chaojie Wang
	Srinivas Peeta
Additional Information:	
Question	Response
The total word count limit is 7500 words including tables. Each table equals 250 words and must be included in your count. Papers exceeding the word limit may be rejected. My word count is:	7299
Is your submission in response to a Call for Papers? (This is not required and will not affect your likelihood of publication.)	No

1	<b>Promoting Multidimensional Equity through Collaborative Routing using Incentive</b>
2	Mechanisms
3	
4	Chaojie Wang
5	School of Civil and Environmental Engineering
6	Georgia Institute of Technology, Atlanta, U.S., 30332
7	Email: chaojie.wang@gatech.edu
8	
9	Srinivas Peeta*
10	School of Civil and Environmental Engineering
11	H. Milton Stewart School of Industrial Engineering
12	Georgia Institute of Technology, Atlanta, U.S., 30332
13	Email: peeta@gatech.edu
14	
15	Word Count: 7,049 words + 1 tables (250 words per table) = 7,299 words
16 17	
18	Submitted to the 2024 Transportation Research Board Annual Meeting for Presentation [July 31 2023]
19	2

<sup>\*</sup> Corresponding author

#### ABSTRACT

1

2

3

4 5

6

7

8

9

10

11 12

13

14

15 16

17 18

19

20

Penalty-based strategies, such as congestion pricing, have been employed to improve traffic network efficiency, but they face criticism for their negative impact on users and equity concerns. Collaborative routing, which allows users to negotiate route choices, offers a solution that considers individual heterogeneity. Personalized incentives can encourage such collaboration and are more politically acceptable than penalties. This study proposes a collaborative routing strategy that uses personalized incentives to guide users towards desired traffic states while promoting multidimensional equity. Three equity dimensions are considered: accessibility equity (equal access to jobs, services, and education), inclusion equity (route suggestions and incentives that do not favor specific users), and utility equity (envy-free solutions where no user feels others have more valuable incentives). The strategy prioritizes equitable access to societal services and activities, ensuring accessibility equity in routing solutions. Inclusion equity is maintained through non-negative incentives that consider user heterogeneity without excluding anyone. An envy-free compensation mechanism achieves utility equity by eliminating envy over incentive-route bundles. A constrained traffic assignment (CTA) formulation and consensus optimization variant are then devised to break down the centralized problem into smaller, manageable parts and a decentralized algorithm is developed for scalability in large transportation networks and user populations. Numerical studies investigate the model's enhancement of equity dimensions and the impact of hyperparameters on system objective tradeoffs and demonstrate the algorithm convergence.

Keywords: accessibility equity, inclusion equity; utility equity; collaborative routing; incentive mechanism

#### INTRODUCTION

#### **Background and motivation**

Congestion pricing mechanisms, employed by traffic operators, aim to enhance transportation system efficiency by targeting macro travel decisions and encouraging alternate modes or timings of travel. Dynamic tolls, as a form of pricing mechanism, influence users' route choices but are penalty-based and disproportionately impact low-income users, thus acting as a regressive tax (1). Existing congestion pricing strategies inadequately address traveler heterogeneity, as the use of user classes (2, 3) obscures individual differences in responses, leading to unmet needs. Such underrepresentation of individual characteristics may result in unintended favoritism, limiting what is termed "inclusion equity." To achieve inclusive consideration of users' interests, traffic operators must promote inclusion equity through personalized interventions that provide non-negative additional utilities.

Personalized behavioral interventions present a complex challenge, as they must address not only increased computational demands and privacy concerns but also potential accusations of discrimination. Users evaluate the personalized options they receive, and interventions must prevent feelings of envy based on utility function assessments, referred to as "utility equity" in this study. The limited exploration of personalized interventions in the literature has left utility equity largely unexamined. To promote inclusion equity by incorporating individual heterogeneities, addressing the challenge of utility equity arising from personalization is essential.

Moreover, prevailing congestion pricing approaches primarily emphasize improving mobility efficiency, aiming to align user equilibrium (UE) flows, which better reflect real-world scenarios, with system optimum (SO) conditions. Although SO conditions offer superior mobility efficiency, they can provoke equity concerns. In SO flow patterns, certain users with identical origins and destinations may encounter considerably longer travel times, resulting in "mobility equity" issues (4). Thus, several studies (4-7) underscore the significance of mobility equity, aiming to minimize travel cost disparities among travelers with matching O-D pairs. The fundamental inquiry concerns whether mobility equity sufficiently captures the true disparities experienced by transportation system users in terms of access and daily functionality. A more pertinent equity goal from a societal standpoint may be "accessibility equity," which emphasizes equal access to job opportunities, services, and resources for all travelers, rather than equal travel times for identical origin-destination trips. Empirical evidence (8) indicates prevalent accessibility inequity within transportation systems. Strategic remedies often proposed to address accessibility inequity include developing efficient public transit networks, encouraging companies to provide transportation subsidies, and coordinating regional housing and economic development (9). Promoting accessibility equity through operational solutions can supplement strategic ones to address systemic equity issues.

In summary, the existing literature on pricing strategies predominantly centers on mobility efficiency through penalty-based system-level approaches. Little attention has been paid to equity concerns, with the focus limited to mobility equity. It also lacks comprehensive research and modeling to address multidimensional equity while factoring heterogeneities in individual user characteristics and needs. Also, the formulation of personalized strategies may exacerbate computational tractability issues due to the explosion in problem dimension. Specifically, if models are to capture individual characteristics, the computational burden increases not only with the size of the network but also with the number of users. Consequently, the modeling and solution design must meet practical requirements when dealing with problems of such high dimension.

To enable equity more comprehensively, we propose the implementation of personalized incentives (in this study, cash or credits that have monetary value) as behavioral interventions, which would influence user route choices at the individual level. This approach, in contrast to penalty-based system-level strategies, considers the specific objectives and limitations of individual users, while simultaneously addressing system-level goals. Also, unlike centralized pricing strategies, the proposed mechanism employs collaborative routing, a more decentralized scheme made possible by emerging connectivity technologies, to ensure computational tractability. In collaborative routing, the traffic operator no longer coordinates

2

3

4

5

6

7

8

9

10

11

12

13 14

15

16

17

18 19

20

21

22

23

24

users' route choices according to system objectives in a centralized manner. Instead, each user works towards their individual contributions to these system objectives while requesting personalized incentives. Thereby, as shown in Figure 1, system objectives are represented as assigned goals to users, and the traffic operator nudges users to work towards these goals individually and voluntarily by providing personalized incentives. Users can negotiate with each other through vehicular on-board units (V2X) or smartphones (P2P networking). In multiple iterations of negotiations, users specify their routing preferences (not the final route choices but the tentative preference for each alternative route during the negotiations), corresponding incentives, and their expectations of other users' routing preferences. Together, they harmonize their individual interests with the assigned goals and the routing preference expectations of other users. That is, each user considers the expectations of routing preferences that other users have of routes this user is willing to consider so as to avoid large deviations from those expectations, and thereby promote consensus. Finally, a consensus is achieved among all users, who follow the consensus routing preferences while receiving the requested incentives from the traffic operator. Compared to a centralized approach, collaborative routing achieves system objectives in a decentralized manner, which decouples the problem dimension explosion issue from the number of users and enables scalable implementation of the proposed mechanisms.

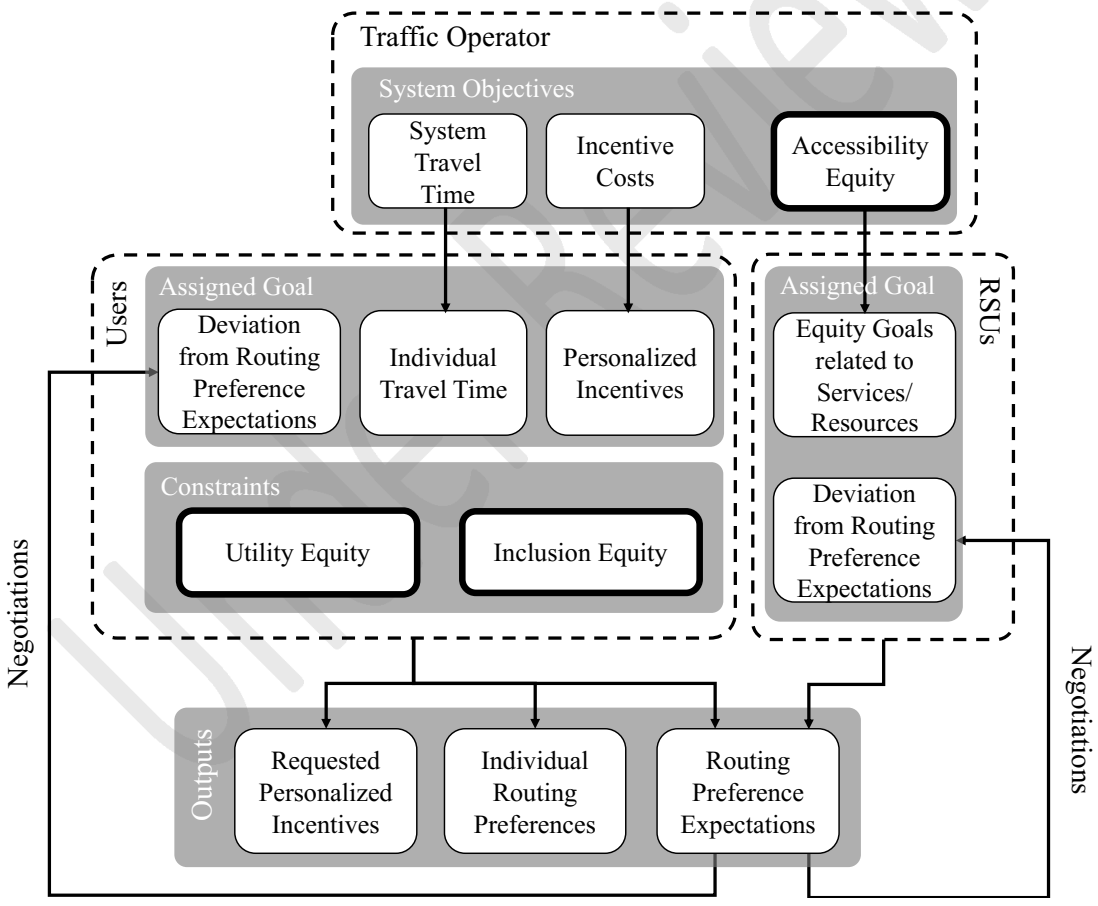


Figure 1: Conceptual framework of the collaborative routing strategy promoting accessibility equity, inclusion equity, and utility equity.

This paper is organized as follows. Section 0 proposes a constrained traffic assignment formulation and highlights its advantages over the network design formulation. Section 0 describes the consensus optimization variant of the constrained traffic assignment formulation and develops a decentralized solution. Numerical studies are presented in Section 0. The paper concludes with a summary of contributions and potential future enhancements in Section 0.

#### CONSTRAINED TRAFFIC ASSIGNMENT FORMULATION

Let us consider a traffic network  $\{N,A\}$ , where N represents the node set, and A denotes the set of directed links. The set of vehicles/users is labeled V. For each individual user  $v \in V$ , the node where it is positioned is its origin  $o_v$ , and its final destination (this is not the local destinations used in the modeling approach) is denoted as  $d_v$ . The alternative route set of user v is  $P_v$ . The routing preference  $f_{p_v}$  is defined as the probability that user v will take route  $p_v$  from  $P_v$ ; thus,  $\sum_{p_v \in P_v} f_{p_v} = 1$ . We assume that users with the same O-D pair have identical alternative route sets. Also, define  $\theta \triangleq \{\theta_{p_v}, p_v \in P_v, v \in V\}$ ,  $f \triangleq \{f_{p_v}, p_v \in P_v, v \in V\}$ . The collaborative routing strategy aims to provide personalized incentives  $\theta_{p_v}$  for each local route  $p_v \in P_v$  for vehicle/user  $v \in V$  to influence the routing preferences and promote the system objectives shown in **Figure 1**.

As depicted in **Figure 2**, the traffic operator proposes routing preferences for users that optimize system objectives, while enabling them to request incentives that facilitate adherence to these preferences. Hence, the decision variables of the upper-level optimization become f, which denotes the users' routing preferences desired by the traffic operator. The lower-level model optimizes  $\theta$ , with the aim of generating the lowest value of incentives necessary to achieve these routing preferences. Specifically, the traffic operator desired routing preferences are fed into the behavioral model of the lower-level optimization, and the required incentives calculated based on these preferences are then used in the upper-level optimization to determine the incentive costs of the system. Therefore, in the constrained traffic assignment formulation, the hat operator is above  $\theta$  as shown in **Figure 2** because incentives are generated by solving the lower-level problem given the desired routing preferences f. This formulation can be viewed as a "constrained" traffic assignment problem undertaken by a traffic operator with a more complex system objective (compared to SO) and more constrained behavioral and incentive requirements (represented by the lower-level model).

Given desired routing preferences f, infer behavioral constraints

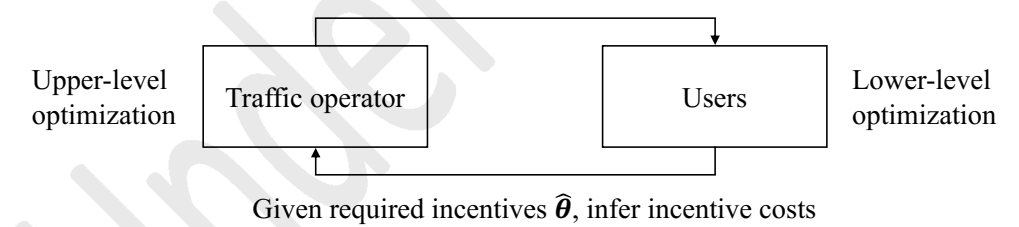


Figure 2: Bi-level structure of the constrained traffic assignment formulation.

#### Incentive cost and mobility inefficiency measures

As illustrated in **Figure 1**, the upper-level optimization model for traffic operators comprises of a tripartite objective function encompassing system mobility efficiency, incentive costs, and accessibility equity. Given the decision variables f, the corresponding required incentives generated by the lower-level optimization model are denoted by the vector  $\hat{\boldsymbol{\theta}}$  (the hat operator indicates that  $\hat{\boldsymbol{\theta}}$  is derived from f), then the expected total incentive costs are:

$$\pi_I = \sum_{v \in V} \sum_{p_v \in P_v} \hat{\theta}_{p_v} f_{p_v}. \tag{1}$$

The expected total system travel time is used as the system mobility inefficiency measure (reducing the mobility inefficiency measure improves mobility efficiency). The probability that user  $v \in V$  uses link  $a \in A$  can be represented using  $\hat{f}_{p_v}$ :

$$x_a^v = \sum_{p_v \in P_v, p_v \ni a} f_{p_v},\tag{2}$$

i.e., the sum of v's routing preferences for routes containing link a. Then, the expected link flows are

$$x_a = \sum_{v \in V} x_a^v = \sum_{v \in V} \sum_{p_v \in P_v} f_{p_v} \delta_{p_v}^a, \tag{3}$$

- where  $\delta_{p_n}^a$  is the link-route indicator variable that is equal to 1 when route  $p_v$  contains link a. The expected
- 3 link travel time of a is  $c_a(x_a)$ , where  $c_a(\cdot)$  is the link performance function of link a (for all  $a \in A$ ;  $c_a(\cdot)$
- 4 are assumed continuous and strictly increasing in this study). The expected route travel time can be
- 5 represented as

9

10

11 12

13

14

15 16

17

18

19 20

21

29

$$t_{p_v} = \sum_{a \in p_v} c_a(x_a). \tag{4}$$

- Note that  $c_a(\cdot)$ ,  $\in p_v$  account for the effect of background traffic and the predicted newly-entering vehicles.
- 7 Thus, Equation (4) does not explicitly incorporate background traffic. Therefore, the expected total system
- 8 travel time is given as

$$\pi_{M} = \sum_{v \in V} \sum_{p_{v} \in P_{v}} t_{p_{v}} f_{p_{v}}.$$
(5)

#### Accessibility inequity measure

To quantify accessibility equity, we must first establish the perfect accessibility equity case, which represents the idealized scenario that we strive to achieve when considering accessibility equity alone. Let us assume that the traffic operator prioritizes equal access to employment, medical services, educational resources, and other societal activities that ought to be accessible to all. We can filter out trips associated with accessing these services/resources from all other trips and categorize them accordingly. Ideally, trips associated with accessing the same type of societal services/resources should have equal expected travel times. For instance, all commuting trips should have the same travel time, and the same applies to trips associated with medical visits. The destinations of such accessibility-sensitive trips are categorized into site groups  $G_i \in G$  based on their service/resource types, where G is the set of all site groups. Then, user groups are defined corresponding to each site group  $G_i$  as  $V_{G_i} \triangleq \{v | v \in V, d_v \in G_i\}$ . This approach enables us to evaluate the inequality in accessibility within  $G_i$  by examining the expected travel time disparity within  $V_{G_i}$ . This study measures the disparity of expected travel times within user group  $V_{G_i}$  as follows:

$$\pi_E^{G_i} = \sum_{v_j \in V_{G_i}} \sum_{v_k \in V_{G_i}} \left( T_{v_j} - T_{v_k} \right)^2, \tag{6}$$

- where  $T_v = \sum_{p_v \in P_v} t_{p_v} f_{p_v}$  is the expected travel time of user  $v \in V_{G_i}$ . Equation (6) is differentiable, making
- 23 it more tractable when integrated in our optimization models. Also, compared to Gini coefficient, Equation
- 24 (6) can better capture the impacts of high expected travel times due to the square operator (de Maio, 2007).
- 25 Then, the system accessibility inequity (minimizing the accessibility inequity measure promotes
- accessibility equity) can be represented as the weighted average of the disparities of all site groups:

$$\pi_E = \sum_{\mathcal{G}_i \in G} \xi_{\mathcal{G}_i} \pi_E^{\mathcal{G}_i},\tag{7}$$

- where  $\xi_{G_i}$  is the weight for site group  $G_i$ , reflecting the importance of accessibility equity of a specific category of societal services/activities from the perspective of the traffic operator  $(\sum_{G_i \in G} \xi_{G_i} = 1)$ .
  - Then the following unit-free objective function is used to represent the traffic operator's objectives:

$$\pi' = \frac{\pi_M + \frac{1}{\lambda} \pi_I}{\pi_{M,0}} + \kappa \frac{\pi_E}{\pi_{E,0}},\tag{8}$$

11

12

13 14

15

16 17

18

19

33

34 35

36

where  $\lambda$  is the traffic operator's "value of time" (i.e., the amount of money that a traffic operator is willing 1 2 to invest to reduce the total system travel time by one unit).  $\pi_{M,0}$  and  $\pi_{E,0}$  are the system mobility 3 inefficiency measure and accessibility inequity measure, respectively, when no behavioral 4 interventions/incentives are applied.  $\kappa$  is an adjustable weight of the mobility equity term. Since there is no incentive cost when no behavioral interventions/incentives are applied,  $\pi_I$  is converted into  $\frac{1}{2}\pi_I$  and 5 benchmarked together with  $\pi_M$  against  $\pi_{M,0}$  to make it unit-free. By adjusting  $\lambda$  and  $\kappa$ , the traffic operator 6 7 can prioritize the three objectives of system efficiency, incentive cost, and accessibility equity according to 8 their preferences.

#### Inclusion equity and utility equity constraints

Inclusion equity imposes a straightforward constraint on the incentives, which requires them to remain non-negative. This encourages users to participate and derive non-negative additional utilities.

Utility equity imposes further constraints on the incentives  $\theta$ . Specifically, it mandates that the expected utility of any user must not be lower than their evaluation of the routing preference-incentive bundles of others who share the same origin-destination pair. This constraint on individual user behavior is similar to the envy-freeness property in (10), which addresses the issue of potential envy among users that could impede their participation. We start by presenting the utility functions of users, which determine how they evaluate a given routing preference-incentive bundle. The utility function consists of two components: individual mobility efficiency and incentive benefits. For a specific route  $p_v \in P_v$ , the utility of user  $v \in V$  can be described as

$$u_v(p_v) = \alpha_v - \beta_v t_{p_v} + \hat{\theta}_{p_v} + \epsilon_{p_v}, \tag{9}$$

where  $\alpha_v$  and  $\beta_v$  are positive parameters capturing the individual characteristics/preferences of user v,  $\epsilon_{p_v}$  is the random term that represents the unobservable or unmeasurable factors of utility (the standard deviations of  $\epsilon_{p_v}$ ,  $p_v \in P_v$ ,  $v \in V$  are 1 in this study), and  $t_{p_v}$  is the expected travel time of route  $p_v$ , which can be calculated using **Equation (4)** (as mentioned before, the hat operator in **Equation (4)** indicates that variables are derived from the equilibrium solution of the lower-level optimization, but calculations apply to non-equilibrium f as well). Then, the expected utility of user  $v \in V$  is given by (11, 12)

$$U_v = \ln \sum_{p_v \in P_v} \exp(\alpha_v - \beta_v t_{p_v} + \widehat{\theta}_{p_v}). \tag{10}$$

Equation (10) describes how user v evaluates their own routing preferences and assigned incentives. How user v assesses the routing preferences and incentives of other users with the same origin and destination is given by

$$U_{v}^{v'} = \ln \sum_{p_{v'} \in P_{v'}} \exp\left(\alpha_{v} - \beta_{v} t_{p_{v'}} + \hat{\theta}_{p_{v'}}\right), v, v' \in V, o_{v} = o_{v'}, d_{v} = d_{v'}.$$
(11)

Note that **Equation (10)** is a special case of **Equation (11)** when  $U_v = U_v^v$ . Then, the utility equity constraints can be represented as

$$U_{v} \ge U_{v}^{v'}, \forall v, v' \in V, o_{v} = o_{v'}, d_{v} = d_{v'}, \tag{12}$$

which ensures that each user  $v \in V$ , utilizing their own utility function, values its own routing preferences and incentives more than those of any other user  $v' \in V$  that shares the same O-D pair.

#### Lower-level equilibrium constraint

In the lower-level problem, by assuming that the random terms in **Equation (9)** are independently and identically distributed (IID), we can define the routing preferences of users through a multinomial logit model:

3 4

5

6

8

9

10

11

12

13

14 15

16 17

18

19

20

21

22

23

24 25

26

$$f_{p_v} = \frac{\exp(\alpha_v - \beta_v t_{p_v} + \hat{\theta}_{p_v})}{\sum_{p_v' \in P_v} \exp(\alpha_v - \beta_v t_{p_v'} + \hat{\theta}_{p_v'})}, p_v \in P_v, v \in V.$$

$$(13)$$

Equations (4) and (13) form a routing preference updating rule. Users communicate their intended routes to the RSUs located within their local ranges. The RSUs, in turn, gather the routing preferences, update  $t_{p_n}$ by applying Equation (4), and disseminate the information within the local range. The users then update their own routing preferences using Equation (13) and share them again. This iterative process continues until equilibrium is achieved, wherein the routing preferences of all users and RSUs reach a stable state of convergence.

#### 7 Bi-level constrained traffic assignment

Combining **Equations (1)-(8)**, the upper-level optimization is as follows:

$$(\mathbf{OPT'}) \min_{f,\theta} \pi' = \frac{1}{\pi_{M,0}} \sum_{v \in V} \sum_{p_v \in P_v} t_{p_v} f_{p_v} + \frac{1}{\lambda \pi_{M,0}} \sum_{v \in V} \sum_{p_v \in P_v} \hat{\theta}_{p_v} f_{p_v} + \frac{\kappa}{\pi_{E,0}} \sum_{\mathcal{G}_i \in G} \xi_{\mathcal{G}_i} \sum_{v_j \in V_{\mathcal{G}_i}} \sum_{v_k \in V_{\mathcal{G}_i}} \left( T_{v_j} - T_{v_k} \right)^2,$$

$$(14.1)$$

$$\mathbf{s.t.} \quad (f, \widehat{\boldsymbol{\theta}}) \in \Phi, \tag{14.2}$$

$$f_{p_v} \ge 0, \forall p_v \in P_v, v \in V, \tag{14.3}$$

$$\sum_{p_v \in P_v} f_{p_v} = 1, \forall v \in V, \tag{14.4}$$

where  $\Phi$  is the feasible region defined by the optimal solution set of the lower-level problem. Unlike in the network design formulation, OPT' only have non-negativity constraints (14.3) and flow conservation constraints (14.4) for routing preferences. Other constraints including the utility equity constraint, incentive non-negativity constraint, and choice behavioral constraint, are all addressed by the lower-level problem and encoded in  $\Phi$ ; that is,  $(f, \hat{\theta}) \in \Phi$  is equivalent to

$$\hat{\theta}_{p_v} \ge 0, \forall p_v \in P_v, v \in V, \tag{15.1}$$

$$U_{v_i}^{v_j}(\widehat{\boldsymbol{\theta}}, \boldsymbol{f}) - U_{v_i}(\widehat{\boldsymbol{\theta}}, \boldsymbol{f}) \le 0, \forall v_i, v_j \in V, o_{v_i} = o_{v_j}, d_{v_i} = d_{v_j},$$
(15.2)

$$f_{p_v} = \frac{\exp(\alpha_v - \beta_v t_{p_v} + \hat{\theta}_{p_v})}{\sum_{p_v' \in P_v} \exp(\alpha_v - \beta_v t_{p_v'} + \hat{\theta}_{p_v'})}, p_v \in P_v, v \in V.$$

$$(15.3)$$

Also, note that in **Equation (14.1)**, the decision variables are f and  $\hat{\theta}$ . Recall that in the network design formulation, there is a 1-to-1 mapping from  $\theta$  to  $\hat{f}$ , and hence equilibrium routing preferences can be represented as  $\hat{f}(\theta)$ . In the following subsections, we analyze the properties of  $\Phi$  and similarly establish a 1-to-1 mapping from f to  $\hat{\theta}$ .

#### Non-emptiness of feasible region $\Phi$

This subsection examines whether there always exists more than one  $\hat{\theta}$  given f, such that  $(f, \hat{\theta}^k) \in$  $\Phi$ . That is, can we always find feasible  $\widehat{\theta}$  given arbitrary f that satisfies **Equations (14.3)** and **(14.4)**? To address this question, the incentives  $\hat{\theta}$  are divided into two parts, logit choice compensations  $\theta^l \triangleq$  $\{\vartheta_{p_v}^l, p_v \in P_v \text{ , } v \in V\}$  and envy compensations  $\boldsymbol{\vartheta}^e \triangleq \{\vartheta_{p_v}^e, p_v \in P_v \text{ , } v \in V\}$ , that is  $\widehat{\boldsymbol{\theta}} = \boldsymbol{\vartheta}^l + \boldsymbol{\vartheta}^e$ 

$$\widehat{\boldsymbol{\theta}} = \boldsymbol{\vartheta}^l + \boldsymbol{\vartheta}^e. \tag{16}$$

The logit choice compensations  $\vartheta^l$  nudge each individual user's routing preferences to the traffic-operator's desired routing preferences f; the envy compensations  $\vartheta^e$  eliminate the envy (in terms of the expected utilities) among users with the same O-D pair.

- **Lemma 1.** Given arbitrary feasible f satisfying **Equations (14.3)** and (14.4), there always exist  $\vartheta^l$ , such 1
- that  $\hat{\boldsymbol{\theta}} = \boldsymbol{\vartheta}^l$  satisfy the non-negativity constraint (15.1) and the behavioral constraint (15.3). 2
- 3
- *Proof.*  $\widehat{\boldsymbol{\theta}} = \boldsymbol{\vartheta}^l$  satisfy the non-negativity constraint (15.1) and the behavioral constraint (15.3). Denote  $\vartheta_v^l \triangleq \min_{p_v \in P_v} \vartheta_{p_v}^l$  and  $p_v^0 \triangleq \arg\min_{p_v \in P_v} \vartheta_{p_v}^l$ , then,  $\delta \vartheta_{p_v}^l = \vartheta_{p_v}^l \vartheta_v^l \geq 0$ . **Equation (15.3)** implies 4

$$f_{p_v} = \exp(\beta_v (t_{p_v^0} - t_{p_v}) + \delta \vartheta_{p_v}^l) f_{p_v^0}, \forall p_v \in P_v, v \in V.$$
(17)

5 Therefore,

$$\vartheta_{p_{v}}^{l} = \vartheta_{v}^{l} + \ln f_{p_{v}} - \ln f_{p_{v}^{0}} + \beta_{v} (t_{p_{v}} - t_{p_{v}^{0}}), \forall p_{v} \in P_{v}, v \in V.$$
(18)

- Hence, for non-negative  $\theta_v^l$ ,  $\theta_{p_v}^l$  defined in **Equation (18)** satisfy the non-negativity constraint (15.1) and 6
- 7 the behavioral constraint (15.3).  $\Box$
- 8 **Lemma 2.** Given arbitrary feasible f satisfying **Equations** (14.3) and (14.4) and  $\vartheta^l$  defined in Equation
- (18), there always exists  $\boldsymbol{\vartheta}^e$ , such that  $\widehat{\boldsymbol{\theta}} = \boldsymbol{\vartheta}^l + \boldsymbol{\vartheta}^e$  satisfy the non-negativity constraint (15.1), utility 9
- 10 equity constraint (15.2) and behavioral constraint (15.3).
- *Proof. With*  $\vartheta^l$  as defined in Equation (18), the non-negativity constraint (15.1) and the behavioral 11
- constraint (15.3) are satisfied. If these two equations should still hold after adding  $\vartheta^e$ ,  $\vartheta^e_{p_y}$  should be of the 12
- same value for all  $p_v \in P_v$ , which is denoted as  $\vartheta_v^e$ . Since  $\vartheta^e$  aim to eliminate the utility disparities among 13
- all users with the same O-D pair, for simplicity, the following proof assumes that  $v_i$  and  $v_i$  have the same 14
- 15 O-D pair. The utility disparities can be quantified as the envy between users. In particular, the envy of user
- 16  $v_i$  for user  $v_i$  can be specified as

$$e_{ij} = U_{v_i}^{v_j} - U_{v_i} = \ln \frac{\sum_{p_{v_j} \in P_{v_j}} \exp\left(\alpha_{v_i} - \beta_{v_i} t_{p_{v_j}} + \hat{\theta}_{p_{v_j}}\right)}{\sum_{p_{v_i} \in P_{v_i}} \exp\left(\alpha_{v_i} - \beta_{v_i} t_{p_{v_i}} + \hat{\theta}_{p_{v_i}}\right)}.$$
(19)

- When  $e_{ij} > 0$ , then user  $v_i$  prefers  $v_j$ 's routing preferences and incentives compared to his/her own ones. 17
- 18 Utility equity implies that for all  $v_i$  and  $v_i$  with the same O-D pair,  $e_{ij} \leq 0$ . We introduce a procedural
- algorithm (10) to achieve utility equity. 19

#### Algorithm 2

20

- 1: for each group of users with the same O-D pairs  $V^{\varrho_k}$ ,  $\varrho_k \in \Theta$ , where  $\Theta$  is the set of O-D pairs.
- Find a user  $v_i \in V^{\varrho_k}$ , such that  $e_{ij} \leq 0$ ,  $\forall v_j \in V^{\varrho_k}$ , and set  $\vartheta_{v_i}^e = 0$ . (see Theorem 1 in (13) for proof of  $v_i$ 's existence).
  - Update the set of non-envious users  $\Gamma^{\varrho_k} = \{v_i | e_{ij} \leq 0, \forall v_i \in V^{\varrho_k}\}$ .
  - repeat until  $\Gamma^{\varrho_k} = V^{\varrho_k}$ . 4:
  - for  $v_i \in V^{\varrho_k} \Gamma^{\varrho_k}$  and  $\max_{v_i \in \Gamma^{\varrho_k}} e_{ij} = \max_{v_j \in V^{\varrho_k}} e_{ij}$ : 5:
  - Set  $\vartheta_{p_{v_i}}^e = \frac{1}{|P_{v_i}|} \max_{v_i \in \Gamma^{\varrho_k}} e_{ij}$ ,  $p_{v_i} \in P_{v_i}$ . 6:
  - 7:
  - Update  $e_{ji}$ ,  $\forall v_j \in V^{\varrho_k}$  using **Equation (19)**. 8:
  - Update the set of non-envious users  $\Gamma^{\varrho_k} = \{v_i | e_{ij} \leq 0, \forall v_j \in V^{\varrho_k}\}$ . 9:
  - 10: end
- Set  $\vartheta_{p_{v_i}}^e = \vartheta_{p_{v_i}}^e + \vartheta_{\varrho_k}^e \forall p_{v_i} \in P_{v_i}, v_i \in V^{\varrho_k}$ , where  $\vartheta_{\varrho_k}^e \ge 0$  is an arbitrary value for each  $\varrho_k \in V^{\varrho_k}$ 11: Θ.

#### 12: end

1 2 3

4

5

8

9

According to Theorem 2 in (13), for a group of users with the same O-D pair  $V^{\varrho_i}$ , such a procedural algorithm can eliminate envy among users within the group in  $|V^{\varrho_i}| - 1$  iterations. Thereby, constraint (15.2) holds for  $\widehat{\boldsymbol{\theta}} = \boldsymbol{\vartheta}^l + \boldsymbol{\vartheta}^e$ . And in lines 5 and 9 of Algorithm 1,  $\vartheta^e_{p_{v_i}} \ge 0$  and  $\vartheta^e_{p_{v_i}} = \vartheta^e_{p'_{v_i}}$  for  $p_{v_i}, p'_{v_i} \in P_{v_i}$ . Therefore, if  $\boldsymbol{\theta}^l$  satisfies constraints (15.1) and (15.3),  $\widehat{\boldsymbol{\theta}} = \boldsymbol{\vartheta}^l + \boldsymbol{\vartheta}^e$  will satisfy constraints (15.1) and (15.3).  $\square$ 

6 **(15.3)**. [7

Lemmas 1 and 2 show that  $\Phi$  is non-empty for arbitrary feasible f satisfying **Equations** (14.3) and (14.4). That is, there are always feasible  $\widehat{\theta}$  to nudge users to any feasible desired f. However, unlike the lower-level equilibrium in the network design formulation, the mapping here from f to  $\widehat{\theta}$  is not 1-to-1.

- 10 **Lemma 3.** If  $(f, \widehat{\theta}^0) \in \Phi$ , then there exist infinite number of  $\widehat{\theta}^k$ , such that  $(f, \widehat{\theta}^k) \in \Phi$ .
- 11 *Proof.* If  $(f, \widehat{\theta}^0) \in \Phi$ , it means that

$$\hat{\theta}_{p_v}^0 \ge 0, \forall p_v \in P_v, v \in V, \tag{20.1}$$

$$U_{v_{i}}^{v_{j}}(\widehat{\boldsymbol{\theta}}^{0}, \boldsymbol{f}) - U_{v_{i}}(\widehat{\boldsymbol{\theta}}^{0}, \boldsymbol{f}) \leq 0, \forall v_{i}, v_{j} \in V, o_{v_{i}} = o_{v_{i}}, d_{v_{i}} = d_{v_{j}},$$
(20.2)

$$f_{p_{v}} = \frac{\exp(\alpha_{v} - \beta_{v}t_{p_{v}} + \hat{\theta}_{p_{v}}^{0})}{\sum_{p_{v}' \in P_{v}} \exp(\alpha_{v} - \beta_{v}t_{p_{v}'} + \hat{\theta}_{p_{v}'}^{0})}, p_{v} \in P_{v}, v \in V,$$
(20.3)

12

Suppose there exists  $\hat{\boldsymbol{\theta}}^k$ , where  $\hat{\theta}^k_{p_v} = \hat{\theta}^0_{p_v} + \Delta^k_{o_v,d_v}(\Delta^k_{o_v,d_v} > 0$  is the same for users with the same O-D pair). Then,

$$\hat{\theta}_{p_v}^k = \hat{\theta}_{p_v}^0 + \Delta_{o_v, d_v}^k > 0, \forall p_v \in P_v, v \in V,$$
(21)

$$\frac{\exp(\alpha_{v} - \beta_{v}t_{p_{v}} + \hat{\theta}_{p_{v}}^{k} + \Delta_{o_{v},d_{v}}^{k})}{\sum_{p_{v}' \in P_{v}} \exp\left(\alpha_{v} - \beta_{v}t_{p_{v}'} + \hat{\theta}_{p_{v}'}^{k} + \Delta_{o_{v},d_{v}}^{k}\right)} = \frac{\exp(\alpha_{v} - \beta_{v}t_{p_{v}} + \gamma_{v}\hat{\theta}_{p_{v}}^{0})}{\sum_{p_{v}' \in P_{v}} \exp\left(\alpha_{v} - \beta_{v}t_{p_{v}'} + \gamma_{v}\hat{\theta}_{p_{v}'}^{0}\right)} = f_{p_{v}}, p_{v} \in P_{v}, v \in V, \tag{22}$$

- which indicates that the incentive non-negativity constraint and choice behavioral constraint hold for  $\hat{\theta}^k$ .
- 16 And for  $\forall v_i, v_j \in V$ ,  $o_{v_i} = o_{v_i}$ ,  $d_{v_i} = d_{v_i}$ ,

$$U_{v_i}^{v_j}(\widehat{\boldsymbol{\theta}}^k, \boldsymbol{f}) = \ln \sum_{p_{v_j} \in P_{v_j}} \exp\left(\alpha_{v_i} - \beta_{v_i} t_{p_{v_j}} + \theta_{p_{v_j}}^k\right)$$

$$= \ln \sum_{p_{v_j} \in P_{v_i}} \exp\left(\alpha_{v_i} - \beta_{v_i} t_{p_{v_j}} + \theta_{p_{v_j}}^0\right) + \left|P_{v_j}\right| \Delta_{o_{v_j}, d_{v_j}}^k,$$
(23)

$$U_{v_i}(\widehat{\boldsymbol{\theta}}^k, \boldsymbol{f}) = U_{v_i}^{v_i}(\widehat{\boldsymbol{\theta}}^k, \boldsymbol{f}) = \ln \sum_{p_{v_i} \in P_{v_i}} \exp\left(\alpha_{v_i} - \beta_{v_i} t_{p_{v_i}} + \gamma_{v_i} \theta_{p_{v_i}}^0\right) + |P_{v_i}| \Delta_{o_{v_i}, d_{v_i}}^k, \tag{24}$$

- where  $|P_{v_i}| = |P_{v_j}|$  (as  $P_{v_i} = P_{v_j}$ ) is the number of alternative routes for their common O-D pair. From
- 18 **Equations (20.2), (23)** and **(24)**, we have

$$U_{v_i}^{v_j}(\widehat{\boldsymbol{\theta}}^0, \boldsymbol{f}) - U_{v_i}(\widehat{\boldsymbol{\theta}}^0, \boldsymbol{f}) \le 0, \forall v_i, v_j \in V, o_{v_i} = o_{v_i}, d_{v_i} = d_{v_i}. \tag{25}$$

- Therefore, the utility equity constraint also holds for  $\hat{\theta}^k$ . Since  $\Delta_{o_v,d_v}^k$ ,  $v \in V$  can be arbitrary positive
- values, there exist infinite number of  $\widehat{\theta}^k$  such that  $(f, \widehat{\theta}^k) \in \Phi$ .  $\square$
- **Theorem 1.**  $(f, \hat{\theta}) \in \Phi$  defines a 1-to-n mapping from f to  $\hat{\theta}$  satisfying **Equations** (14.3) and (14.4).
- 22 *Proof.* Lemma 1 and Lemma 2 prove the existence of the mapping. And Lemma 3 shows that it is 1-to-n.
- **23** [

#### Single-level constrained traffic assignment

- Theorem 1 makes  $\hat{\theta}$  a necessary part of the decision variables in **OPT**'. To eliminate  $\hat{\theta}$  from the
- decision variables and reduce the problem dimension by half, a 1-to-1 mapping from f to  $\hat{\theta}$  is established.
- 4 First, replace constraint (14.2) in **OPT**' with the following lower-level optimization problem.

$$\widehat{\boldsymbol{\theta}} = \underset{\boldsymbol{\theta}, \text{s.t.}(f, \boldsymbol{\theta}) \in \Phi}{\text{arg min}} \sum_{v \in V} \sum_{p_v \in P_v} \theta_{p_v} f_{p_v}. \tag{26}$$

- 5 Lemma 4. Replacing constraint (14.2) with Equation (26) does not change the local optimal solutions of
- 6 *OPT*′.

1

7 Proof. Suppose  $(f^*, \widehat{\theta}^*) \in \Phi$  are local optimal solutions of **OPT**', which implies that

$$\pi'(f^*, \widehat{\theta}^*) \le \pi'(f^* + \delta f, \widehat{\theta}^* + \delta \widehat{\theta})$$
(27)

8 for all  $\delta f$  and  $\delta \widehat{\theta}$  with small  $l_2$  norms. Let  $\delta f = 0$ , then

$$\pi'(\mathbf{f}^*, \widehat{\boldsymbol{\theta}}^*) \le \pi'(\mathbf{f}^*, \widehat{\boldsymbol{\theta}}^* + \delta\widehat{\boldsymbol{\theta}}), \tag{28}$$

9 which reduces to

$$\sum_{v \in V} \sum_{p_v \in P_v} \theta_{p_v}^* f_{p_v} \le \sum_{v \in V} \sum_{p_v \in P_v} (\theta_{p_v}^* + \delta \theta_{p_v}) f_{p_v}. \tag{29}$$

- 10 Therefore,  $\hat{\theta}^*$  satisfies Equation (26) as well, which means that changing constraint (14.2) to Equation
- 11 (26) does not exclude any local optimal solutions of OPT'.  $\square$
- 12 **Lemma 5.** Equation (26) defines a 1-to-1 mapping from f to  $\hat{\theta}$  satisfying Equations (14.3) and (14.4).
- 13 Proof. According to Lemma 6 in (13), if  $\vartheta_{\varrho_k}^e = 0$ ,  $\varrho_k \in \Theta$ , then Algorithm 1 determines unique and
- minimum non-negative  $\boldsymbol{\vartheta}^e$  given  $\boldsymbol{f}$  and  $\boldsymbol{\vartheta}^l$ , which defines a 1-to-1 mapping:  $\boldsymbol{\vartheta}^e(\boldsymbol{f},\boldsymbol{\vartheta}^l)$ . Using Equation
- 15 (18), we have

$$\sum_{v \in V} \sum_{p_v \in P_v} \theta_{p_v} f_{p_v} = \sum_{\varrho_k \in \Theta} \sum_{v \in V^{\varrho_k}} \left( |p_v| (\vartheta_v^l + \vartheta_v^e) f_{p_v} + \sum_{p_v \in P_v} (\vartheta_{p_v}^l - \vartheta_v^l) f_{p_v} \right), \tag{30}$$

- where  $\vartheta_v^e = \vartheta_{p_v}^e$ ,  $p_v \in P_v$  (line 11 in Algorithm 1 indicates that  $\vartheta_{p_v}^e$ ,  $\forall v \in V$  have the same value, which is
- 17 denoted as  $\vartheta_{v}^{e}$  here).
- Let  $\tilde{\vartheta}_{p_v}^l \triangleq \vartheta_{p_v}^l \vartheta_v^l, \forall p_v \in P_v, v \in V$  and  $\tilde{\vartheta}^e(f, \tilde{\vartheta}^l)$  be the corresponding envy compensations
- 19 generated using Algorithm 1 with  $\vartheta_{\varrho_k}^e = 0$ . According to **Equation (18)**,  $\tilde{\vartheta}^l$  is deterministic. Also, as
- 20  $\widetilde{\vartheta}^e(f,\widetilde{\vartheta}^l)$  are the unique minimum non-negative envy compensations,

$$\sum_{\varrho_{k}\in\Theta} \sum_{v\in V^{\varrho_{k}}} \left( |p_{v}| (\vartheta_{v}^{l} + \vartheta_{v}^{e}) f_{p_{v}} + \sum_{p_{v}\in P_{v}} (\vartheta_{p_{v}}^{l} - \vartheta_{v}^{l}) f_{p_{v}} \right) \\
\geq \sum_{\varrho_{k}\in\Theta} \sum_{v\in V^{\varrho_{k}}} \left( |p_{v}| (\tilde{\vartheta}_{v}^{e}) f_{p_{v}} + \sum_{p_{v}\in P_{v}} \tilde{\vartheta}_{p_{v}}^{l} f_{p_{v}} \right).$$
(31)

- Equations (30) and (31) indicate that  $\tilde{\boldsymbol{\theta}} = \tilde{\boldsymbol{\vartheta}}^e + \tilde{\boldsymbol{\vartheta}}^l$  is a unique minimizer of Equation (26), and thus
- defines a 1-to-1 mapping from f to  $\widehat{\theta}$  satisfying Equations (14.3) and (14.4).  $\square$
- Then, we can specify the following constrained traffic assignment formulation with a bi-level
- structure and show its equivalence to *OPT'*.

$$(\mathbf{BOPT'}) \min_{f} \pi' = \frac{1}{\pi_{M,0}} \sum_{v \in V} \sum_{p_v \in P_v} t_{p_v} f_{p_v} + \frac{1}{\lambda_0 \pi_{M,0}} \sum_{v \in V} \sum_{p_v \in P_v} \hat{\theta}_{p_v} f_{p_v} + \frac{\kappa}{\pi_{E,0}} \sum_{g_i \in G} \xi_{g_i} \sum_{v_j \in V_{g_i}} \sum_{v_k \in V_{g_i}} \left( T_{v_j} - T_{v_k} \right)^2,$$
(32.1)

3

4

13

14

15

16

17

$$\mathbf{s.t.} \quad \widehat{\boldsymbol{\theta}}(\boldsymbol{f}) = \underset{\boldsymbol{\theta}, \mathbf{s.t.}(\boldsymbol{f}, \boldsymbol{\theta}) \in \Phi}{\text{arg min}} \sum_{v \in V} \sum_{p_v \in P_v} \theta_{p_v} f_{p_v'}, \tag{32.2}$$

$$f_{p_v} \ge 0, \forall p_v \in P_v, v \in V, \tag{32.3}$$

$$\sum_{p_v \in P_v} f_{p_v} = 1, \forall v \in V, \tag{32.4}$$

While the lower-level optimization problem defines a 1-to-1 mapping from f to  $\hat{\theta}$ , there is no closed-form function to represent it. Algorithm 1 is a procedural algorithm, and thus  $\hat{\theta}(f)$  is non-differentiable, which does not aid solution algorithm design. According to Theorem 4 in (13), the sum of envy compensations of user group  $V^{\varrho_k}$  is bounded on the upper side; that is,

$$\sum_{v_i \in V^{\varrho_k}} \sum_{p_{v_i} \in P_{v_i}} \vartheta_{pv_i}^e \le \sum_{v_i \in V^{\varrho_k}} \ln \sum_{p_{v_i} \in P_{v_i}} \exp\left(\alpha_{v_i} - \beta_{v_i} t_{p_{v_i}} + \vartheta_{pv_i}^l\right) = \bar{\vartheta}_{\varrho_k}^e. \tag{33}$$

However, using **Equation (18)** to calculate  $\theta^l(f)$  also makes  $\hat{\theta}(f)$  non-differentiable. Therefore, the minimization operator in **Equation (18)** can be smoothened as follows.

$$\vartheta_{v}^{l} \triangleq \min_{p_{v} \in P_{v}} \vartheta_{p_{v}}^{l} \approx -\frac{1}{K} \ln \left( \sum_{p_{v} \in P_{v}} \exp(-K\vartheta_{p_{v}}^{l}) \right), \tag{34}$$

$$p_{v}^{0} \triangleq \underset{p_{v} \in P_{v}}{\operatorname{arg \, min}} \, \vartheta_{p_{v}}^{l} \approx \left[ \frac{\exp\left(-K\vartheta_{pv_{i}}^{l}\right)}{\sum_{p_{v_{j}} \in P_{v}} \exp\left(-K\vartheta_{pv_{j}}^{l}\right)} \middle| p_{v_{i}} \in P_{v} \right] \cdot \left[ p_{v_{i}} \middle| p_{v_{i}} \in P_{v} \right]^{T}. \tag{35}$$

7 Therefore, the constrained traffic assignment model (CTA) can be represented as follows:

$$(\mathbf{CTA}) \min_{\mathbf{f}} \pi' = \frac{1}{\pi_{M,0}} \sum_{v \in V} \sum_{p_v \in P_v} t_{p_v} f_{p_v} + \frac{1}{\lambda \pi_{M,0}} \left( \sum_{v \in V} \sum_{p_v \in P_v} \vartheta_{p_v}^l(\mathbf{f}) f_{p_v} + \sum_{\varrho_k \in \Theta} \bar{\vartheta}_{\varrho_k}^e(\mathbf{f}, \boldsymbol{\vartheta}^l) \right) + \frac{\kappa}{\pi_{E,0}} \sum_{\mathcal{G}_i \in G} \xi_{\mathcal{G}_i} \sum_{v_j \in V_{\mathcal{G}_i}} \sum_{v_k \in V_{\mathcal{G}_i}} \left( T_{v_j} - T_{v_k} \right)^2,$$

$$(36.1)$$

$$\mathbf{s.\,t.} \quad \sum_{p_v \in P_v} f_{p_v} = 1, \forall v \in V, \tag{36.2}$$

$$f_{p_v} \ge \epsilon, \forall p_v \in P_v, v \in V, \tag{36.3}$$

Note that formulation (49.1)-(49.3) does not generate individual envy compensations, but only the upper bound of the sum of envy compensations of each user group  $\varrho_k$ ,  $\bar{\vartheta}^e_{\varrho_k}$ . Hence, the individual envy compensations are obtained using the following two steps: (i) generate the unique minimum envy compensation  $\tilde{\vartheta}^e_{p_v}$ ,  $p_v \in P_v$ ,  $v \in \varrho_k$  following Algorithm 1; and (ii) distribute the remaining group envy compensations,  $\bar{\vartheta}^e_{\varrho_k} - \sum_{v \in \varrho_k} \sum_{p_v \in P_v} \tilde{\vartheta}^e_{p_v}$ , to each alternative of each user within the user group equally.

#### DECENTRALIZED SOLUTION ALGORITHM

This section first derives a consensus optimization formulation (COCTA) based on CTA defined in Equations (36.1)-(36.3), which allows us to develop a decentralized solution algorithm to enable computational tractability in large-scale implementations. Denote the feasible region of routing preferences defined by Equations (36.2) and (36.3) as  $\Omega$ .

$$(\textbf{COCTA}) \min_{f, \{f^{\varrho_k}\}, \{f^{\varrho_k}\}, \{f^{\varrho_k}\}} \Pi = \frac{1}{\pi_{M,0}} \sum_{v \in V} \sum_{p_v \in P_v} t_{p_v}(f^v) f_{p_v}^v$$
(37.1)

$$+\frac{1}{\lambda \pi_{M,0}} \left( \sum_{v \in V} \sum_{p_v \in P_v} \vartheta_{p_v}^l(\boldsymbol{f}^v) f_{p_v}^v + \sum_{\varrho_k \in \Theta} \bar{\vartheta}_{\varrho_k}^e(\boldsymbol{f}^{\varrho_k}, \boldsymbol{\vartheta}^l(\boldsymbol{f}^{\varrho_k})) \right) \\ + \frac{\kappa}{\pi_{E,0}} \sum_{\mathcal{G}_i \in G} \xi_{\mathcal{G}_i} \sum_{v_j \in V_{\mathcal{G}_i}} \sum_{v_k \in V_{\mathcal{G}_i}} \left( T_{v_j}(\boldsymbol{f}^{\mathcal{G}_i}) - T_{v_k}(\boldsymbol{f}^{\mathcal{G}_i}) \right)^2,$$

s.t. 
$$f \in \Omega$$
, (37.2)

$$\mathbf{f}^{v}, \mathbf{f}^{\varrho_{k}}, \mathbf{f}^{g_{i}} \in \mathbf{\Omega}, \forall v \in V, \varrho_{k} \in \Theta, \mathcal{G}_{i} \in G$$

$$(37.3)$$

$$\mathbf{f} = \mathbf{f}^{v} = \mathbf{f}^{\varrho_k} = \mathbf{f}^{\varrho_i}, \forall v \in V, \varrho_k \in \Theta, \mathcal{G}_i \in G$$
(37.4)

- 1 Lemma 6. COCTA is equivalent to CTA.
- 2 Proof. Replace  $f^v$ ,  $f^{\varrho_k}$ ,  $f^{g_i}$  in  $\Pi$  with f, then constraints (37.3) and (37.4) can be removed and  $f^v$ ,  $f^{\varrho_k}$ ,  $f^{g_i}$
- 3 can be eliminated from the decision variables. Then, **COCTA** becomes **CTA**.  $\square$
- The objective function (37.1) of **COCTA** can be reorganized as follows:

$$\Pi = \sum_{v \in V} \sum_{p_v \in P_v} \left( \frac{1}{\pi_{M,0}} t_{p_v}(\mathbf{f}^v) f_{p_v}^v + \frac{1}{\lambda \pi_{M,0}} \vartheta_{p_v}^l(\mathbf{f}^v) f_{p_v}^v \right) 
+ \sum_{\varrho_k \in \Theta} \left( \frac{1}{\lambda \pi_{M,0}} \bar{\vartheta}_{\varrho_k}^e (\mathbf{f}^{\varrho_k}, \boldsymbol{\vartheta}^l(\mathbf{f}^{\varrho_k})) \right) 
+ \sum_{g_i \in G} \frac{\kappa \xi_{g_i}}{\pi_{E,0}} \sum_{v_j \in V_{G_i}} \sum_{v_k \in V_{G_i}} \left( T_{v_j}(\mathbf{f}^{g_i}) - T_{v_k}(\mathbf{f}^{g_i}) \right)^2.$$
(38)

5 Let

$$g_{\nu}(f^{\nu}) = \sum_{p_{\nu} \in P_{\nu}} \left( \frac{1}{\pi_{M,0}} t_{p_{\nu}}(f^{\nu}) f_{p_{\nu}}^{\nu} + \frac{1}{\lambda \pi_{M,0}} \vartheta_{p_{\nu}}^{l}(f^{\nu}) f_{p_{\nu}}^{\nu} \right), \tag{39}$$

$$g_{\varrho_k}(\mathbf{f}^{\varrho_k}) = \frac{1}{\lambda \pi_{M,0}} \bar{\vartheta}_{\varrho_k}^e (\mathbf{f}^{\varrho_k}, \boldsymbol{\vartheta}^l(\mathbf{f}^{\varrho_k})), \tag{40}$$

$$g_{g_i}(\mathbf{f}^{g_i}) = \frac{\kappa \xi_{g_i}}{\pi_{E,0}} \sum_{v_i \in V_{G_i}} \sum_{v_k \in V_{G_i}} \left( T_{v_j}(\mathbf{f}^{g_i}) - T_{v_k}(\mathbf{f}^{g_i}) \right)^2, \tag{41}$$

6 Then

9

$$\Pi = \sum_{v \in V} g_v(\mathbf{f}^v) + \sum_{\varrho_k \in \Theta} g_{\varrho_k}(\mathbf{f}^{\varrho_k}) + \sum_{\mathcal{G}_i \in G} g_{\mathcal{G}_i}(\mathbf{f}^{\mathcal{G}_i}). \tag{42}$$

7 Incorporating constraints (37.4) into the objective function gives us the augmented Lagrangian:

$$\mathcal{L}_{\text{COCTA}}(f, \{f^{v}|v \in V\}, \{f^{\varrho_{k}}|\varrho_{k} \in \Theta\}, \{f^{g_{i}}|G_{i} \in G\}) 
= \sum_{v \in V} \left(g_{v}(f^{v}) + \langle \boldsymbol{\eta}^{v}, f^{v} - f \rangle + \frac{\rho_{v}}{2} ||f^{v} - f||^{2}\right) 
+ \sum_{\varrho_{k} \in \Theta} \left(g_{\varrho_{k}}(f^{\varrho_{k}}) + \langle \boldsymbol{\eta}^{\varrho_{k}}, f^{\varrho_{k}} - f \rangle + \frac{\rho_{\varrho_{k}}}{2} ||f^{\varrho_{k}} - f||^{2}\right) 
+ \sum_{g_{i} \in G} \left(g_{g_{i}}(f^{g_{i}}) + \langle \boldsymbol{\eta}^{g_{i}}, f^{g_{i}} - f \rangle + \frac{\rho_{g_{i}}}{2} ||f^{g_{i}} - f||^{2}\right).$$
(43)

8 Then, the following algorithm can be used to solve **COCTA**.

Algorithm 3

1: Initialize the decision variables  $f_{(0)}$ ,  $\{f_{(0)}^{v}|v\in V\}$ ,  $\{f_{(0)}^{\varrho_{k}}|\varrho_{k}\in\Theta\}$ ,  $\{f_{(0)}^{g_{i}}|G_{i}\in G\}$  and dual variables  $\{\eta_{(0)}^{v}|v\in V\}$ ,  $\{\eta_{(0)}^{\varrho_{k}}|\varrho_{k}\in\Theta\}$ ,  $\{\eta_{(0)}^{g_{i}}|G_{i}\in G\}$ . Set  $r\leftarrow0$ ;

2: repeat until the convergence criteria are met.

3: Update 
$$f_{(r+1)} = \underset{f \in \Omega}{\operatorname{argmin}} \mathcal{L}_{\operatorname{COCTA}} \left( f, \left\{ f_{(r)}^{v} \right\}, \left\{ f_{(r)}^{g_i} \right\}, \left\{ \eta_{(r)}^{v} \right\}, \left\{ \left\{ \eta_{(r)}^{g_i} \right\} \right\} \right)$$
.

4: Update 
$$f_{(r+1)}^v = \underset{f^v}{\operatorname{argmin}} g_v(f^v) + \langle \eta_{(r)}^v, f^v - f_{(r+1)} \rangle + \frac{\rho_v}{2} \left| \left| f^v - f_{(r+1)} \right| \right|^2$$
,  $\forall v \in V$ .

5: Update 
$$f_{(r+1)}^{\varrho_k} = \underset{f^{\varrho_k}}{\operatorname{argmin}} g_{\varrho_k}(f^{\varrho_k}) + \langle \boldsymbol{\eta}_{(r)}^{\varrho_k}, f^{\varrho_k} - f_{(r+1)} \rangle + \frac{\rho_{\varrho_k}}{2} \left| \left| f^{\varrho_k} - f_{(r+1)} \right| \right|^2$$
,  $\forall \varrho_k \in \Theta$ .

6: Update 
$$f_{(r+1)}^{\mathcal{G}_i} = \min_{f^{\mathcal{G}_i}} g_{\mathcal{G}_i}(f^{\mathcal{G}_i}) + \langle \boldsymbol{\eta}_{(r)}^{\mathcal{G}_i}, f^{\mathcal{G}_i} - f_{(r+1)} \rangle + \frac{\rho_{g_i}}{2} \left| \left| f^{\mathcal{G}_i} - f_{(r+1)} \right| \right|^2$$
,  $\forall \mathcal{G}_i \in \mathcal{G}$ .

7: Update 
$$\boldsymbol{\eta}_{(r+1)}^{v} = \boldsymbol{\eta}_{(r)}^{v} + \rho_{v} (\boldsymbol{f}_{(r+1)}^{v} - \boldsymbol{f}_{(r+1)}), \forall v \in V; \ \boldsymbol{\eta}_{(r+1)}^{\varrho_{k}} = \boldsymbol{\eta}_{(r)}^{\varrho_{k}} + \rho_{\varrho_{k}} (\boldsymbol{f}_{(r+1)}^{\varrho_{k}} - \boldsymbol{f}_{(r+1)}), \forall \varrho_{k} \in \Theta; \ \boldsymbol{\eta}_{(r+1)}^{g_{i}} = \boldsymbol{\eta}_{(r)}^{g_{i}} + \rho_{g_{i}} (\boldsymbol{f}_{(r+1)}^{g_{i}} - \boldsymbol{f}_{(r+1)}), \forall g_{i} \in G.$$

8: Set  $r \leftarrow r + 1$ .

9: end

Algorithm 2 has an iterative structure. In each iteration, both the consensus variables  $f_{(r)}^{v}$  and the local variables  $f_{(r)}^{v}$ ,  $f_{(r)}^{\varrho_k}$  are updated. Specifically, the consensus variables are updated by minimizing the augmented Lagrangian that uses the local variables in the previous iteration. As the name suggests, the optimization in line 3 aims to create a consensus among the local variables (eventually, they should have the same values as implied by constraint (37.4)). Note that though the optimization problem in line 3 has the same dimension as **CTA**, it has a more standard quadratic programming form, which can be solved as follows:

$$f_{(r+1)} = \operatorname{proj}_{\boldsymbol{a}} \left[ \frac{\sum_{v \in V} \left( \rho_{v} \boldsymbol{f}_{(r)}^{v} + \boldsymbol{\eta}_{(r)}^{v} \right) + \sum_{\varrho_{k} \in \Theta} \left( \rho_{\varrho_{k}} \boldsymbol{f}_{(r)}^{\varrho_{k}} + \boldsymbol{\eta}_{(r)}^{\varrho_{k}} \right) + \sum_{\mathcal{G}_{i} \in G} \left( \rho_{\mathcal{G}_{i}} \boldsymbol{f}_{(r)}^{\mathcal{G}_{i}} + \boldsymbol{\eta}_{(r)}^{\mathcal{G}_{i}} \right)}{\sum_{v \in V} \rho_{v} + \sum_{\varrho_{k} \in \Theta} \rho_{\varrho_{k}} + \sum_{\mathcal{G}_{i} \in G} \rho_{\mathcal{G}_{i}}} \right]$$

$$= \operatorname{proj}_{\boldsymbol{a}} \boldsymbol{z}_{(r)}$$

$$(44)$$

Note that the feasible set  $\Omega$  is an affine half space  $\{f^0|Af^0=1, f^0\geq 0\}$  (here  $Af^0=1$  is the matrix form of  $\sum_{p_v\in P_v}f^0_{p_v}=1, \forall v\in V$ ), which allows us to represent  $f^0_{(r+1)}$  as:

$$f_{(r+1)} = \operatorname{proj}_{\Omega} \mathbf{z}_{(r)} = \left[ \mathbf{z}_{(r)} - \mathbf{A}^{T} \left( \mathbf{A} \mathbf{A}^{T} \right)^{-1} \left( \mathbf{A} \mathbf{z}_{(r)} - \mathbf{1} \right) \right]_{\epsilon +}, \tag{45}$$

where the  $[\cdot]_{\epsilon+}$  operator applies max $\{\cdot, \epsilon\}$  to each element of the vector. As **Equation (45)** is composed solely of elementary linear algebra, the consensus updating step in line 3 of Algorithm 2 is considerably inexpensive in practice.

The local variables are updated by solving local optimization problems, which has simpler objective functions and optimize a local copy of f. The local objective functions are simpler not only because  $g_v$ ,  $g_{\varrho_k}$ ,  $g_{g_i}$  are small components of  $\Pi$ , but also because the problem dimension is greatly reduced though  $f^v$ ,  $f^{\varrho_k}$ ,  $f^{g_i}$  have the same dimension as f. For example, consider the optimization at line 4 in Algorithm 2. As **Equation (39)** shows,  $g_v(f^v)$  are represented using  $t_{p_v}$ ,  $\vartheta_{p_v}^l$ ,  $f_{p_v}^v$ ,  $p_v \in P_v$ . And according to **Equations (18)**, (34), and (35),  $\vartheta_{p_v}^l$  is represented using  $t_{p_v}$ ,  $p_v \in P_v$ . Then, for  $v_i$ ,  $v_i \in V$ ,

$$\frac{\partial g_{v_i}}{\partial f_{p_{v_j}}^{v_i}} = \sum_{p_{v_i} \in P_{v_i}} \frac{\partial g_{v_i}}{\partial t_{p_{v_i}}} \cdot \frac{\partial t_{p_{v_i}}}{\partial f_{p_{v_j}}^{v_i}} + \sum_{p_{v_i} \in P_{v_i}} \frac{\partial g_{v_i}}{\partial f_{p_{v_i}}^{v_i}} \cdot \frac{\partial f_{p_{v_i}}^{v_i}}{\partial f_{p_{v_j}}^{v_i}} + \sum_{p_{v_i} \in P_{v_i}} \frac{\partial g_{v_i}}{\partial \theta_{p_{v_i}}^{v_i}} \cdot \sum_{p'_{v_i} \in P_{v_i}} \frac{\partial \theta_{p_{v_i}}^l}{\partial t_{p'_{v_i}}} \cdot \frac{\partial t_{p'_{v_i}}}{\partial f_{p_{v_j}}^{v_i}},$$

$$(46)$$

Therefore, if  $p_{v_i}$  and  $p_{v_j}$  share no links, then  $\frac{\partial t_{p_{v_i}}}{\partial f_{p_{v_j}}^{v_i}} = 0$ ,  $\forall p_{v_i} \in P_{v_i}$ ;  $\frac{\partial f_{p_{v_i}}^i}{\partial f_{p_{v_j}}^{v_i}} = 0$ ,  $\forall p_{v_i} \in P_{v_i}$ , and thus  $\frac{\partial g_{v_i}}{\partial f_{p_{v_j}}^{v_i}} = 0$ 

#### Wang and Peeta

0. This further implies that in the solution to the local optimization problem,  $f_{p_{v_i}(r+1)}^{v_i} = f_{p_{v_i}(r+1)}$ . Just as the toy example in Section 4.1 shows, when updating  $f_{(r+1)}^{v}$ , most of the elements can simply be copied from  $f_{(r+1)}$ . The "effective" decision variables of the local optimization problem are the routing preferences that affect  $t_{p_v}, p_v \in P_v$ . The label "local optimization" is partly because these routing preferences are either from user v or some neighboring users (whose alternative routes have at least one shared link with any of the alternative routes of v). Another reason for this label is that it is intended to be solved by user v. In real world implementations, these local optimizations are performed by the computing units on CAVs or the smart phones of users.

#### NUMERICAL STUDIES

#### Data preparation and experiment settings

Table 1 summarizes the specifications of the three traffic networks used in this study, and their layouts are shown in Figure 3. Since the proposed strategies generate personalized routing preferences and incentives for each user, using the original O-D demand data<sup>1</sup> for these networks exceeds typically available computational resources. That is, though in practice the decentralized algorithm will run concurrently on thousands of computing units (of users' phones or their vehicles), we employ a single computer with many threads to simulate this procedure. Therefore, though the proposed algorithm scales well with problem size in the real world, the study experiments cannot generate individual routing preferences and incentives for millions of users. To limit problem size, we reduce the total number of users while maintaining the original O-D demand distributions. For instance, **Figure 3**(b) visualizes the demand distributions among the 24 nodes in the Sioux Falls network (**Figure 3**(a)). The original demand is 360,600. Users are generated with a 0.1% probability, resulting in 362 users and 219 active O-D pairs (i.e., O-D pairs with positive demands). In addition, the capacity parameters in the link performance functions are changed to replicate comparable congestion levels. The capacity parameters of all links in the Sioux Falls network are multiplied by 1/3000. The numbers of active O-D pairs, generated users, and the corresponding capacity coefficients used in the Anaheim network (**Figure 3**(c)) and the Chicago Sketch network (**Figure 3**(d)) are also listed in Table 1.

Table 1. Specifications of networks and demands.

_	# of	# of	# of	# of	Total #	Average # of	Average # of	Capacity
Network	nodes	edges	ODs	users	of paths	links per path	neighboring paths	coeff.
Sioux Falls	24	76	219	362	438	4.25	181.92	1/3000
Anaheim	416	914	417	995	834	17.31	381.67	1/300
Chicago Sketch	993	2950	1522	1932	3044	8 09	198 42	1/1200

<sup>&</sup>lt;sup>1</sup> https://github.com/bstabler/TransportationNetworks

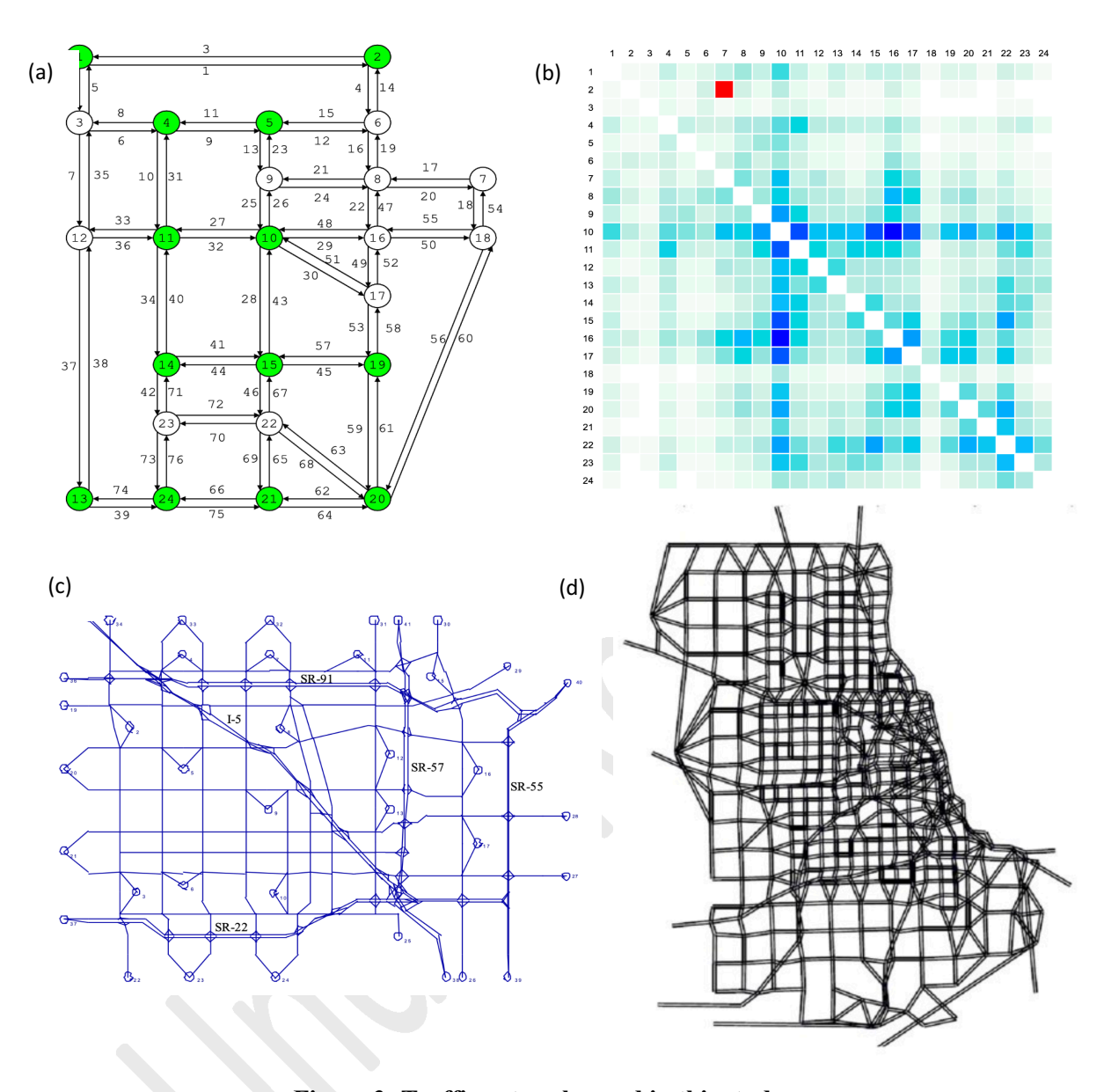


Figure 3: Traffic networks used in this study.

For each network, two nodes are selected as societal service/resource-related sites, forming two user groups  $V_{G_i}$ . Specifically, for the Sioux Falls network, users heading to nodes 8 and 11 are categorized into two separate user groups for accessibility inequity measures; for the Anaheim network, nodes 6 and 15 are selected; and for the Chicago Sketch network, nodes 8 and 11 are selected. The weights  $\xi_{G_i}$  are set to 1. For each user v,  $\alpha_v$  is randomly sampled from a uniform distribution U(0,10), and  $\beta_v$  is randomly sampled from U(0.002,0.004). Note that the units for travel times, incentives, and these parameters are omitted in the numerical studies as the objective function in **Equation (38)** is designed to be unit-free.  $\rho_v$ ,  $v \in V$ ,  $\rho_{\rho_k}$ ,  $\rho_k \in \Theta$ ,  $\rho_{G_i}$ ,  $G_i \in G$  are all set to 1000.  $\epsilon$  in **Equation (36.3)** is set to 0.001.

As a benchmark, original equilibrium routing preferences are computed using the method of successive averages when behavioral interventions are not considered (that is, no incentives). The corresponding mobility inefficiency measure  $\pi_{M,0}$  and accessibility inequity measure  $\pi_{E,0}$  in the objective function are calculated. **Figure 4** depicts the optimal solutions for the three objectives with different  $\lambda$  and

 $\kappa$  for the Sioux Falls network. As **CTA** is a non-linear, non-convex optimization problem, the optimal solutions denote the best ones from among 10 repetitions of Algorithm 2 with the same settings.

### 4 Effectiveness in promoting mobility efficiency and three dimensions of equity

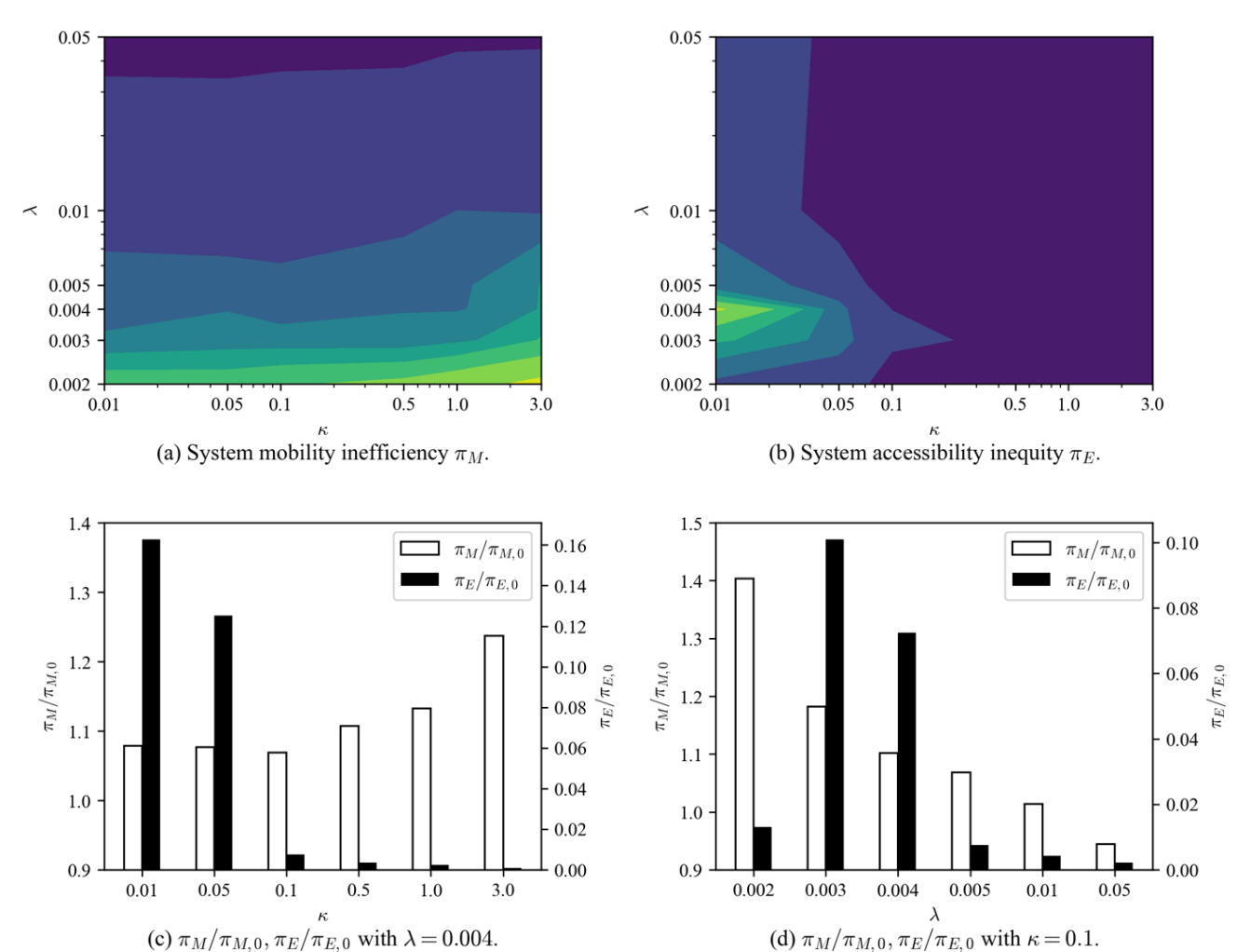


Figure 4: System mobility inefficiency and accessibility inequity tradeoffs: (a) and (b) illustrate  $\pi_M$  and  $\pi_E$ , respectively, for different  $\kappa$  and  $\lambda$  (lighter colors indicate higher values); (c) and (d) plot  $\pi_M/\pi_{M,0}$  and  $\pi_E/\pi_{E,0}$  for fixed  $\lambda$  and  $\kappa$ , respectively.

The insights for system accessibility can be summarized as follows:

- The mobility inefficiency measure  $\pi_M$  increases with  $\kappa$ . This indicates that as the traffic operator prioritizes accessibility equity more, system efficiency can be slightly lowered. However, the sensitivity of  $\pi_M$  to changes in  $\kappa$  is comparatively lower than that of  $\lambda$ , which is illustrated in Figure 4(a) (the contour lines are almost parallel to the  $\kappa$  axis when  $\kappa$  is small). This is because  $\kappa$  is designed to balance the tradeoff between  $\pi_E/\pi_{E,0}$  and  $\left(\pi_M + \frac{1}{\lambda}\pi_I\right)/\pi_{M,0}$ . As a result,  $\pi_M$  does not change as much as  $\pi_E$  when  $\kappa$  changes because a decrease in  $\pi_M$  increases  $\pi_I$ , which moderates the overall reduction in  $\pi_M + \frac{1}{\lambda}\pi_I$ .
- Figure 4(b) shows that system accessibility inequity decreases significantly with increase in  $\kappa$  as indicated by the deepening hues along the x-axis. This can be attributed to the traffic

- operator's increased prioritization of achieving accessibility equity at the expense of mobility efficiency and incentive costs. Figure 4(c) illustrates similar tendencies in the percentage changes of  $\pi_E/\pi_{E,0}$  with changes in  $\kappa$ .
- However, the trend of  $\pi_E$  observed with changes in  $\lambda$  is not straightforward. As depicted in Figure 4(b) and Figure 4(d), both  $\pi_E$  and  $\pi_E/\pi_{E,0}$  initially increase with  $\lambda$ , reaching a peak near  $\lambda=0.003$ , before decreasing with further increases in  $\lambda$ . Note that  $\beta_v, v \in V$  range from 0.002 to 0.004, which implies that the average value of time of users is around 0.003. When the traffic operator's value of time  $\lambda$  falls below the average value of time of users, the travel time savings are generally not worth the invested incentives from the traffic operator's perspective. This is because travelers request more incentives than expected as they value time more highly than the traffic operator.

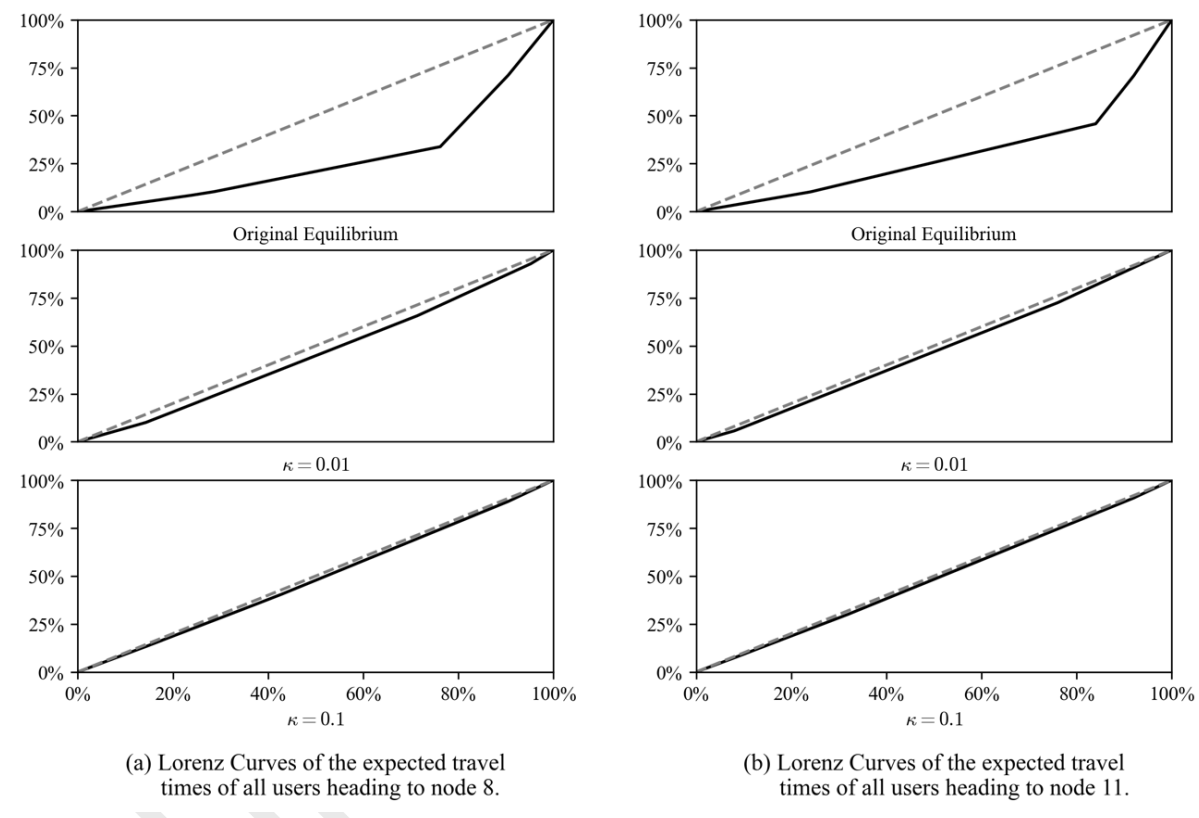


Figure 5: Lorenz Curves of the expected travel times for societal service/resource-related nodes in the Sioux Falls network (x axes are the user percentage by travel time distributions; y axes are cumulative shares of total travel time).

To evaluate the effectiveness of the proposed collaborative routing strategy in terms of promoting equitable access to societal services/activities, the Lorenz curves of the expected travel times of users heading to nodes 8 and 11 in the Sioux Falls network are shown in **Figure 5**. Nodes 8 and 11 are assumed to provide two different societal services/resources; thereby users heading to them form two user groups for accessibility inequity measures. The Lorenz curve is widely used to illustrate income/wealth distributions. The Lorenz curve here shows how the percentage share of the total group travel time changes as the percentage share of users by travel time distributions increases. It is also closely related to the Gini coefficient; the gray dashed line connecting (0%, 0%) and (100%, 100%) denotes perfect accessibility equity and the Gini coefficient is the ratio of the area between the Lorenz curve (solid black line) and the gray dashed line to the area between the gray dashed line and the x axis. Both **Figure 5**(a) and 10(b) show

that the Lorenz curves are closer to the perfect accessibility equity line as  $\kappa$  increases, indicating that the accessibility equity of both groups of users is enhanced.

### Efficiency evaluation of the decentralized algorithm (Algorithm 2)

**Figure 6** depicts the convergence performance of Algorithm 2. Figs. 11(a), 11(b) and 11(c) illustrate the trajectories of objective function (37.1) in the first 1000 iterations in the Sioux Falls, Anaheim, and Chicago Sketch networks, respectively. The red dashed lines denote the objective function value of the original equilibrium state (without behavior interventions) as benchmark. The results indicate that Algorithm 2 can identify acceptable solutions to the non-linear non-convex problem (**COCTA**) rather quickly; that is, 200-600 iterations to exceed the benchmark. But many more iterations may be required to find a good solution as the reduction in the objective function value greatly slows down with the number of iterations. Figure 6(d) shows that the convergence rate slows down when more users participate in the decentralized algorithm as it is harder to reach a consensus for a larger group of users. However, for all three networks, Algorithm 2 converges to a good solution within 1000 iterations, which is acceptable for practical deployment (each iteration takes tens milliseconds).

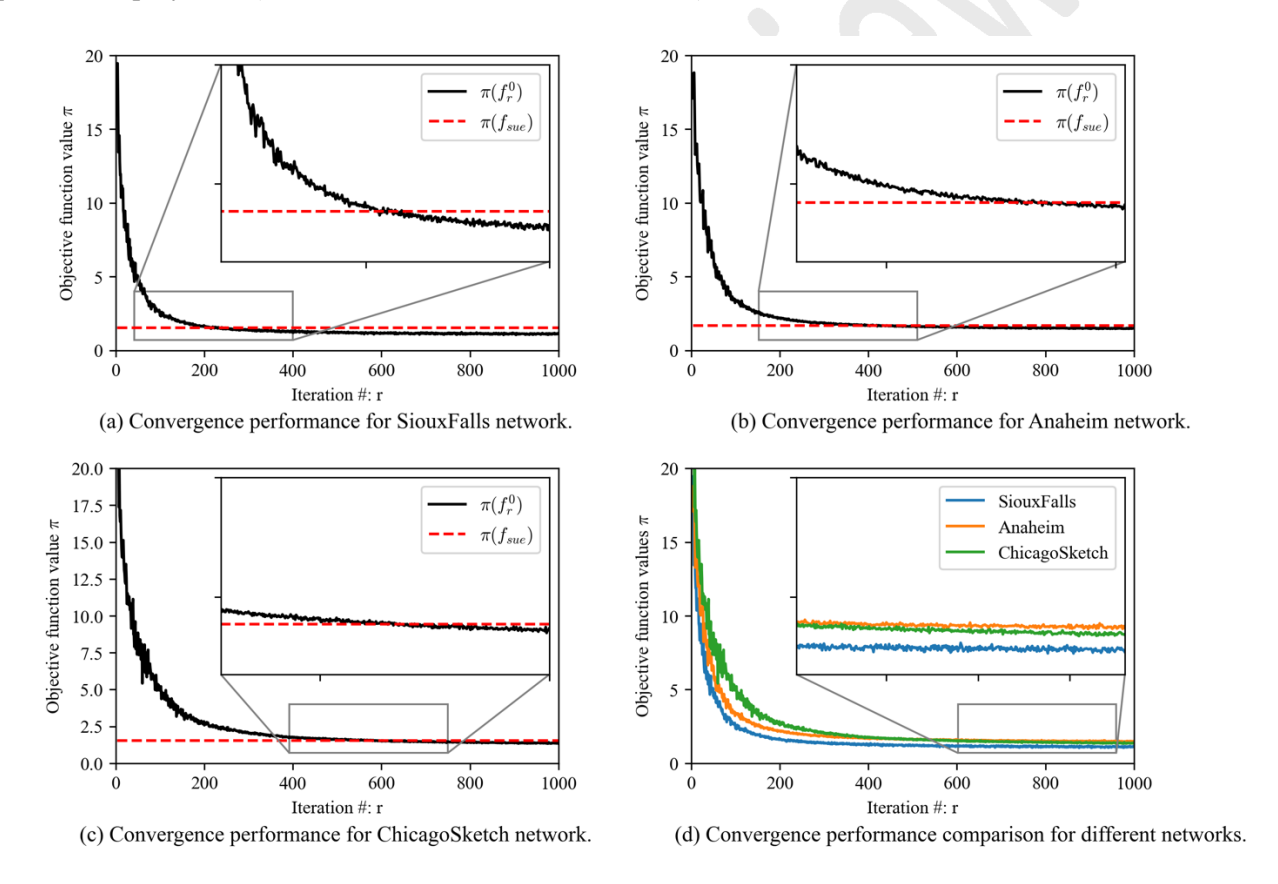
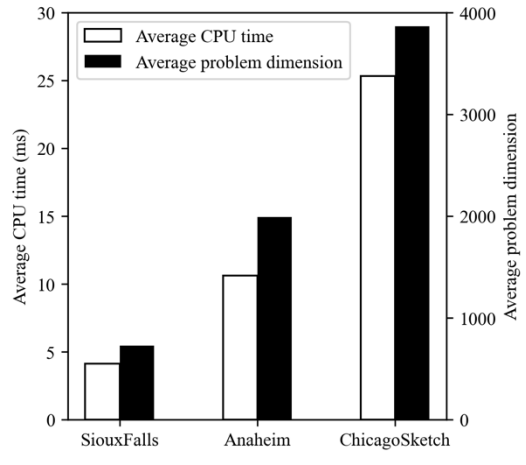
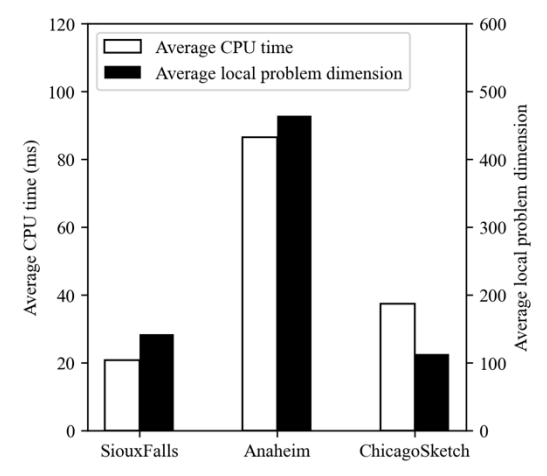


Figure 6: Convergence performance of Algorithm 2.





(a) Average CPU times of the consensus step for different networks. (b) Average CPU times of the local updating steps for different networks.

Figure 7: Computational times of Algorithm 2.

The computational performance of Algorithm 2 is evaluated using the average CPU times of the consensus step (line 3 in Algorithm 2) and the local optimization steps (lines 4, 5, and 6 in Algorithm 2). **Figure 7**(a) shows that the average computational time of the consensus step in all 1000 iterations of the Sioux Falls network increases with problem dimension (i.e., the dimension of routing preferences f) as line 3 of Algorithm 2 is not executed in a decentralized manner in the experiments. However, **Equations (44)** and **(45)** indicate that each element of  $f_{(r+1)}$  can be updated locally in practice. Updating different elements of  $f_{(r+1)}$  locally reduces the computational time of the consensus step, while also distributing the communication load and reduce physical transmission distance and communication delays.

Figure 7(b) illustrates that the average computational times of the local updating steps (lines 4, 5, and 6 in Algorithm 2) are closely related to the average dimension of the local optimization problems (the local optimization problem for each user/RSU can have different dimensions). While the average local problem dimension and average CPU time increase significantly for the Anaheim network compared to the Sioux Falls network, the same is not true for the Chicago Sketch network. The average dimension of local optimization problems in the Chicago Sketch network is similar to that of the Sioux Falls network, leading its average CPU time for local updating steps to be slightly higher than that of the Sioux Fall network. This can be explained by the network statistics in Table 1; though the Chicago Sketch network has the largest numbers of nodes, edges, paths, and users, its average number of links per path (8.09) is much smaller than that of the Anaheim network (17.31). Hence, its paths are less coupled in terms of shared links and similar to those of the Sioux Falls network as indicated by the average number of neighboring paths. Note that the average number of neighboring users is directly related to the dimensions of local optimization problems as shown in Section 0, and is proportional to the average number of neighboring paths. Hence, this illustrates that the computational load of each computing unit in the proposed decentralized algorithm does not scale directly with network size or number of users. Instead, it depends more on the average dimension of local optimization problems.

#### **CONCLUDING COMMENTS**

To our knowledge, this study pioneers the integration of multidimensional equity considerations in traffic networks, reflecting user behavior and network context. It introduces collaborative routing strategies through incentive mechanisms, promoting equity in three dimensions. Firstly, the model accounts for accessibility equity, a recognized societal target in planning, but rarely addressed operationally. By producing routing outcomes sensitive to access equity, our strategy tackles this crucial dimension of traffic system inequity. Secondly, the incentive mechanism incorporates utility equity, a scarcely explored

constraint in incentive personalization, ensuring incentives do not provoke envy or perceived inequity, thus enhancing their practical appeal. Thirdly, inclusion equity is addressed by utilizing personalized incentives to shape user routing preferences, imposing non-negativity requirements reflecting realistic individual participation willingness. The resulting complexity due to multiple equity dimensions renders centralized solutions impractical, necessitating a decentralized approach for computational tractability.

This study systematically integrates multidimensional equity considerations into the analytical modeling and quantitative analysis of collaborative routing strategies. Future research directions include: (i) using more comprehensive discrete choice models to accurately model users' route choice behavior; (ii) exploring the impact of path generation strategies on the proposed path-based model and its efficacy in promoting equity; (iii) incorporating the heterogeneity in the value of time in users' utilities to reflect their individual characteristics more accurately; (iv) extending the framework to dynamic traffic assignment to better capture traffic dynamics; and (v) incorporating more cost-efficient types of incentives in the proposed strategies.

#### **ACKNOWLEDGMENTS**

This study is supported by the National Science Foundation (NSF) Smart and Connected Communities (SCC) grant #2125390, and by Georgia Institute of Technology. Any errors or omissions remain the sole responsibility of the authors.

#### **AUTHOR CONTRIBUTIONS**

The authors confirm contribution to the paper as follows: study conception and design: Chaojie Wang, Srinivas Peeta; data collection: Chaojie Wang; analysis and interpretation of results: Chaojie Wang; draft manuscript preparation: Chaojie Wang, Srinivas Peeta. All authors reviewed the results and approved the final version of the manuscript.

#### **REFERENCES**

- 1. Schweitzer, L., & Taylor, B. D. (2008). Just pricing: The distributional effects of congestion pricing and sales taxes. *Transportation*, 35(6), 797–812.
- 2. Kumar, V., Bhat, C.R., Pendyala, R.M., You, D., Ben-Elia, E., Ettema, D., 2016. Impacts of incentive-based intervention on peak period traffic: Experience from the Netherlands. *Transportation Research Record*, 2543, 166-175.
- Jahn, O., Möhring, R. H., Schulz, A. S., & Stier-Moses, N. E. (2005). System-Optimal Routing of Traffic Flows with User Constraints in Networks with Congestion. *Operations Research*, 53(4), 600– 616.
- 5. Angelelli, E., Morandi, V., Savelsbergh, M., & Speranza, M. G. (2021). System optimal routing of traffic flows with user constraints using linear programming. *European Journal of Operational Research*, 293(3), 863–879.
- 41 6. Angelelli, E., Morandi, V., & Speranza, M. G. (2018). Congestion avoiding heuristic path generation for the proactive route guidance. *Computers & Operations Research*, 99, 234–248.
- Jalota, D., Solovey, K., Tsao, M., Zoepf, S., & Pavone, M. (2021). Balancing Fairness and Efficiency
   in Traffic Routing via Interpolated Traffic Assignment. *Proceedings of the International Joint Conference on Autonomous Agents and Multiagent Systems*, 2, 678–686.
- Liu, X., Lin, Z., Huang, J., Gao, H., & Shi, W. (2021). Evaluating the inequality of medical service accessibility using smart card data. *International Journal of Environmental Research and Public Health*, 18(5), 2711-2722.
- 9. Gordon, P., Kumar, A., & Richardson, H. W. (1989). The influence of metropolitan spatial structure on commuting time. *Journal of Urban Economics*, 26(2), 138-151.

#### Wang and Peeta

10

- 1 10. Wang, C., Peeta, S., & Wang, J. (2021). Incentive-based decentralized routing for connected and autonomous vehicles using information propagation. *Transportation Research Part B: Methodological*, 149, 138–161.
- 4 11. Small, K. A., & Rosen, H. S. (1981). Applied Welfare Economics with Discrete Choice Models. *Econometrica*, 49(1) 105-130.
- Williams, H. C. W. L. (1977). On the Formation of Travel Demand Models and Economic Evaluation
   Measures of User Benefit. *Environment and Planning A: Economy and Space*, 9(3), 285-344.
- 13. Haake, C. J., Raith, M. G., & Su, F. E. (2002). Bidding for envy-freeness: A procedural approach to n-player fair-division problems. *Social Choice and Welfare*, 19(4), 723-749.